The Confinement of High Temperature Plasma by the Heliotron Magnetic Fields

AUTHOR(S):

UO, Kōji

The Confinement of High Temperature Plasma by the Heliotron Magnetic Fields

By

Kōji Uo*

(Received October 31, 1961)

A magnetic field named the Heliotron field is produced by electric current in a series of pair coils wound around a discharge tube at regular intervals. The electric current in each coil of the pair differs both in intensity and direction. The lines of force in this field undulate near the tube axis without cutting the wall, while those near the tube wall intersect the wall. Thus a high temperature plasma can be produced by ohmic heating in the central region of this field, and the plasma is prevented from touching the wall. This field is found to satisfy the necessary condition for equilibrium. The interchange instability of the plasma confined in this field is discussed. A general expression is given for the magnetic field, and it is shown that the Heliotron B magnetic field, the cylindrical cusp field, the helical winding field of the Stellarater and the Picket-Fence field are derived as special cases of this general formula.

§ 1. Introduction

There are two different type situations in the confinement of high temperature plasma by a magnetic field. The magnetic pressure is comparable with the plasma pressure in the one and much larger than the plasma pressure in the other. For example, the pinch type machine belongs to the first type and the mirror type machine and the stellarator to the second.

Recently two machines of the second type have been constructed successively at Kyoto University and named the Helliotron *A* and the Heliotron *B*.[1,5] The Heliotron** magnetic field uses a series of pair coils which are wound around a discharge tube of toroidal shape at regular intervals. In general, the electric currents in the coils of each pair are different in both intensity and direction. The magnetic field produced by these currents is composed of two different regions. In the region near the tube axis the magnetic lines of force undulate along the axis without cutting the wall, whereas those near the tube wall cross

* Department of Electrical Engineering

** The basic plan of the Heliotron field was first presented at the meeting of Thermonuclear Conference of Japan (May 5, 1958), and was published in Kakuyūgō Kenkū, **1**, 20 (1958).

the boundary and make short arcs inside the wall. Therefore, a high-temperature plasma can be produced by ohmic heating only in the central region of the magnetic field, since particles near the wall cannot be accelerated sufficiently by the applied axial electric field. Thus it may be said that the machine has the effect of preventing the hot plasma from directly touching the wall.

There are two sorts of Heliotron magnetic fields. One is axisymmetrical and is called the Heliotron *B* field, and the other is helically invariant and is called the Heliotron *H* field. The distinctive characteristics of the Heliotron *B* field are as follows:

(1) The charge separation of the plasma could be eliminated by the azimuthal drift of the particles in the undulated field.

(2) By the existence of the circular cusp series inside the tube wall, we can satisfy the necessary condition for equilibrium of the plasma under the magnetohydrodynamical assumption.

(3) The plasma in this field is stable for the interchange instability under a proper gradient of the plasma density.

(4) It seems possible that the magnetic mirrors in the Heliotron field will prevent generation of runaway electrons.

(5) It is possible to heat the plasma by the generation of ioncyclotron waves using the beach effect at many slopes of the undulation of the Heliotron field.

(6) The configuration of the Heliotron field is very flexible. By changing the current ratio of one coil series to another, we may obtain various magnetic field configurations from the ZETA type field to the Picket Fence type field. And we need not worry too much over the exactness of the field configuration, since we can bore apertures for observation without introducing field correction coils.

(7) The lines of force near the wall in themselves make a plasma diameter limiter. Therefore the metal aperture limiter is not necessary.

The main defects of the Heliotron *B* field are:

(1) The stability condition for interchange instability seems rater too strict.

(2) The particles will be lost from the circular cusp series. However, the former faults will be overcome in the Heliotron *H* field. The Heliotron *H* magnetic field can be obtained by making the coils of the Heliotron *B* (Fig. 2.4) helical around the tube as shown in Fig. 2.7. This field is like the field produced by the helical windings of the stellarators making the pitch of the windings shorter than the stellarator and the current flowing in the windings different from each other. Thus we can make the rotationally transformed field

the same as the stellarator and make a plasma which is stable for interchange instability. Furthermore in the Heliotron H field, the field intensities, B_ρ, B_θ and B_z, have comparable orders. Therefore, when the magnetic field is sufficiently strong, it seems that the distortion of the Hiliotron H field by the plasma current would be very small, and that the field could confine the plasma with β nearly equal to unity. Making $\lambda=1$, the Heliotron H field becomes the helical Picket Fence field.

The Heliotron A of toroidal shape was constructed first. Its discharge tube was made of Zircon ceramic with a torus radius of 30 cm, the inner radius of the tube being 8 cm, and the thickness of the tube wall 1 cm. It had six apertures for observation. Unfortunately the Heliotron A was damaged, presumably due to the residual stress in the ceramic and the mechanical stress caused by the field coils which were wound around the torus tube.

Next, the Heliotron B was constructed. Its discharge tube has the shape of a race-track and is made of stainless steel. Its curved part has nearly the same size as the Heliotron A, and the length of its straight part is 50 cm, the inner radius of the tube is 8.4 cm~7.5 cm, and the wall thickness 0.2 cm. It has nine apertures for observation. The field intensity is about 10,000~16,000 gausses. Various experiments are being carried out with the Heliotron B at present.

In this paper, we describe first the configuration of the Heliotron magnetic field and discuss the conditions for the confinement of a high temperature plasma in this field. Secondly, it will be shown that this field satisfies the necessary conditions for equilibrium within the framework of the magnetohydrodynamic approximation. Lastly, we will discuss the interchange instability of plasma in this field.

§2. General Configuration of the Heliotron Magnetic Field

Let us consider a magnetic field produced by an electric current in the coils, which are wound, as shown in Fig. 2.1, around a torus tube at regular intervals. The outline of the magnetic field in a cylindrical section involving the tube axis is shown graphically in Fig. 2.2.

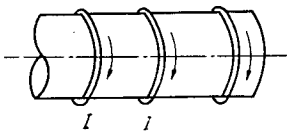

Fig. 2.1

It is assumed that the charged particles in the slightly ionized gas in the tube move along the lines of force, being accelerated by an electric field, and that the plasma is so dilute and the magnetic field is so strong that the magnetic pressure p_{mag} is much larger than the plasma pressure p_{gas}. In this case charged particles inside the curve AB of Fig. 2.2 are accelerated over a long distance and reach a high energy. On the other hand, particles outside AB run along

the lines of force which are interupted by the tube wall and therefore cannot attain a high energy. Thus it may be expected that we can generate the discharge only in the region inside the curve because the electric conductivity along the x direction becomes so poor near the wall that the high temperature plasma in the inner region is prevented from reaching the wall except at the point G (see Fig. 2.2).

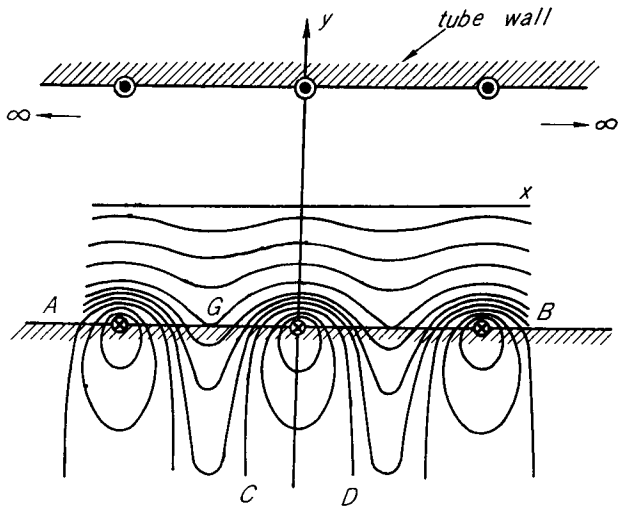

Fig. 2.2 The lines of force inside the curve AB undulate along the axis without cutting the wall, whereas those outside the curve AB cross the wall and those outside CD are the leakage flux.

This field appears to be effective for protecting the wall against the hot plasma and for decreasing the influx of impurity from the wall. At point G however, the high temperature plasma touches the wall. In order to correct this defect, double rows of coils as shown in Figs. 2.3 and 2.4 are introduced. The direction of the electric current in the outer coils is opposite to that of the inner one. The magnetic lines of force in these fields are roughly sketched in Figs. 2.5 and 2.6.

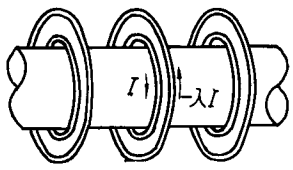

Fig. 2.3

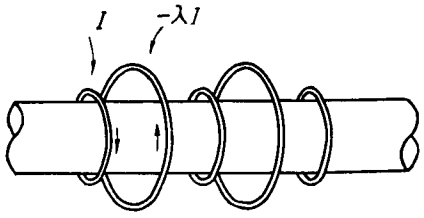

Fig. 2.4

In these fields the magnetic lines of force inside *AMB* do not touch the wall, whereas all lines outside *AMB* enter the wall leaving short arcs inside the wall. The lines of force near the axis are completely separated from those near the wall, and therefore the high temperature plasma confined by the lines of force inside *AMB* do not touch the wall at all. Therefore, these fields are evidently more advantageous for confining hot plasma than the field shown in Fig. 2.2.

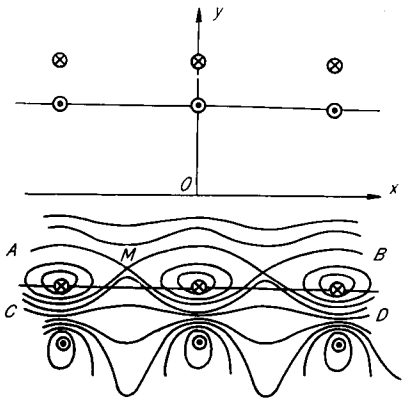

Fig. 2.5

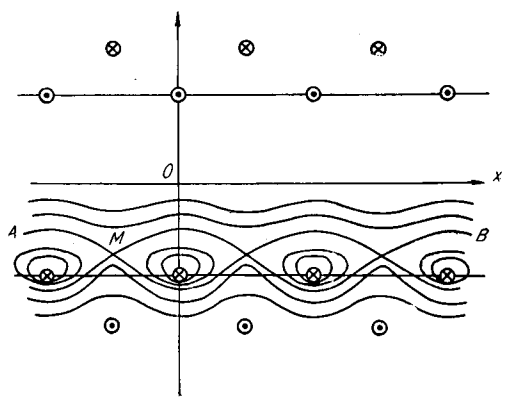

Fig. 2.6

The rows of coils in Fig. 2.4 may be modified as shown in Fig. 2.7, or coils may be wound helically around the tube as shown in Figs. 2.8~2.10. In the latter case the lines of force also become helical, and this field may be called the Heliotron *H* field.

The magnetic fields generated by these double rows of coils are named the Heliotron magnetic field. Let us denote the ratio of the electric currents in the two coils of a pair by λ. If we put $\lambda=1$ in the windings of Figs. 2.7 and 2.10, they reduce to the Picket Fence field and to the field produced by the helical windings of the Stellarator respectively.

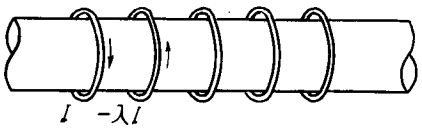

Fig. 2.7

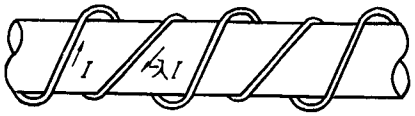

Fig. 2.9

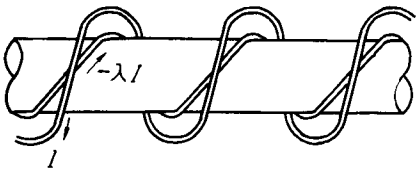

Fig. 2.8

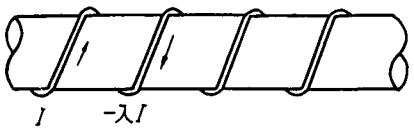

Fig. 2.10

It is one of the merits of the Heliotron field that we can bore apertures for observation without introducing correction coils, which are usually necessary for eliminating the field distortion caused by the irregularity of the coils near the apertures.

The patterns of the magnetic fields produced by the windings are observed experimentally by the iron sand method, and their pictures are shown in Figs. 2.11~2.19.

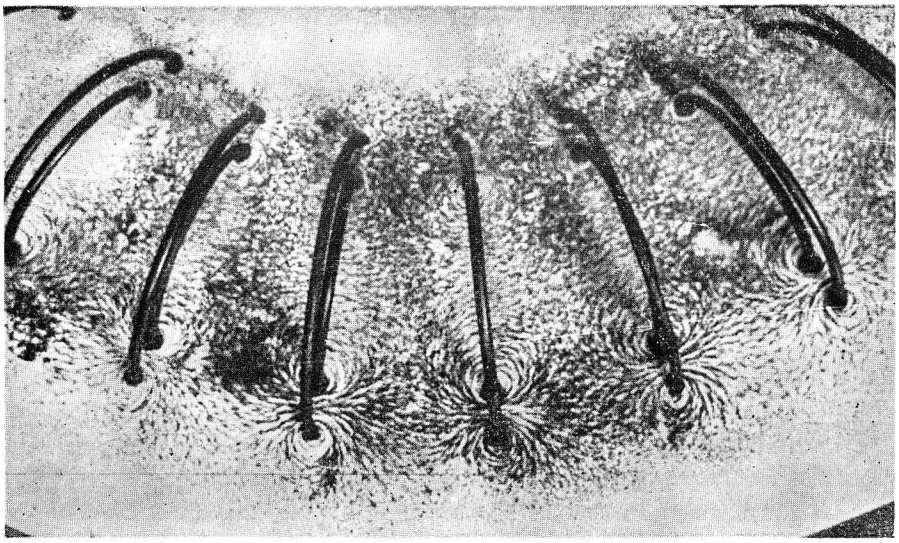

Fig. 2.11. The Heliotron A Magnetic Field Produced by the Coils Shown in Figs. 2.3 and 2.5.

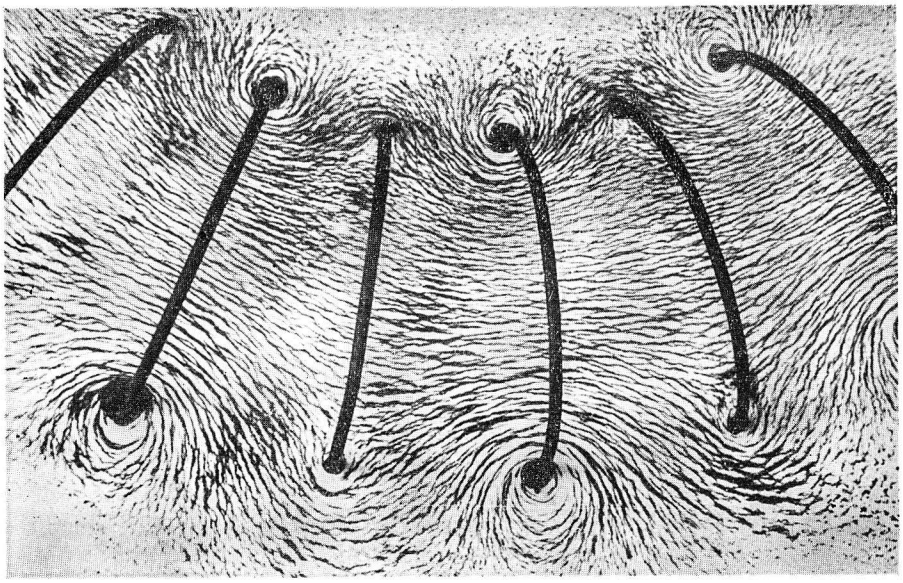

Fig. 2.12. The Heliotron B Magnetic Field $\lambda=0.17$.

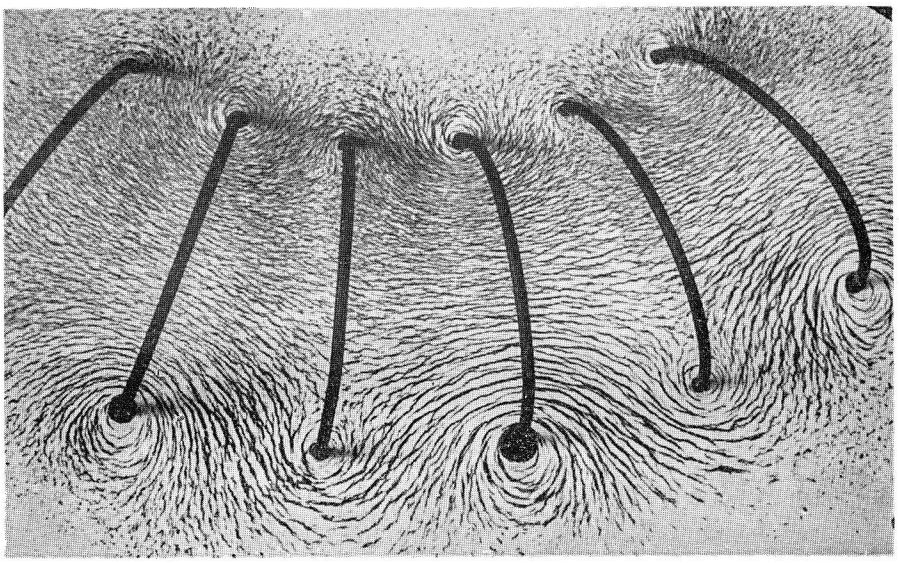

Fig. 2.13. The Heliotron B Magnetic Field $\lambda=0.33$.

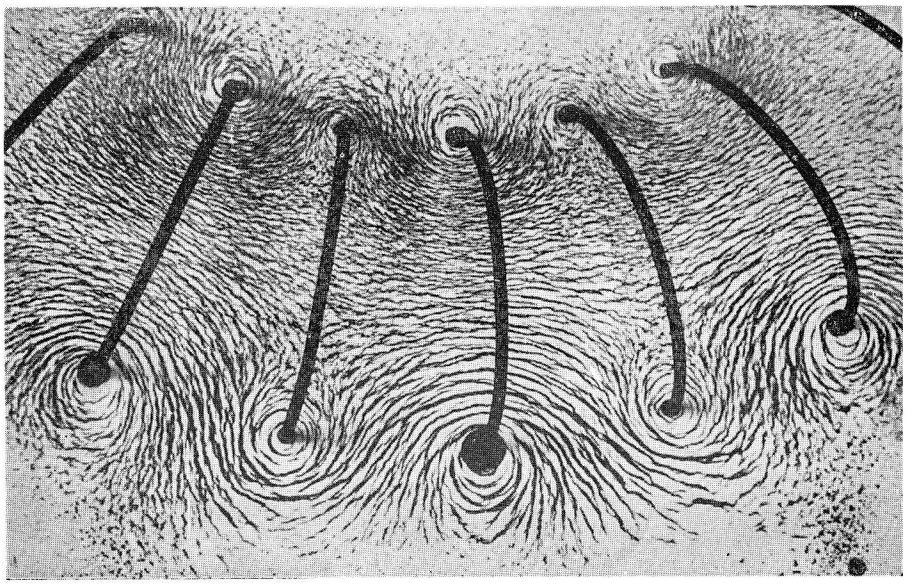

Fig. 2.14. The Heliotron B Magnetic Field $\lambda=0.50$.

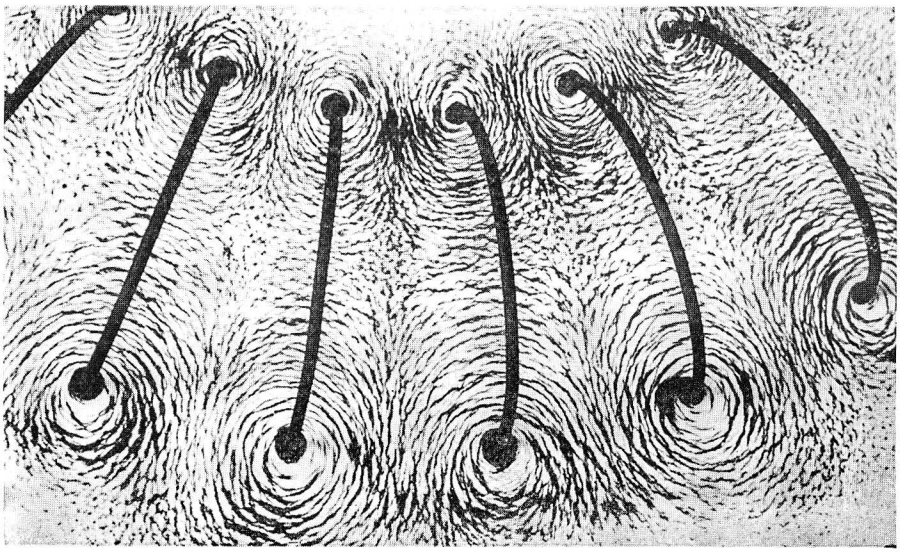

Fig. 2.15. The Heliotron B Magnetic Field $\lambda=1.00$.
(The Picket Fence Field)

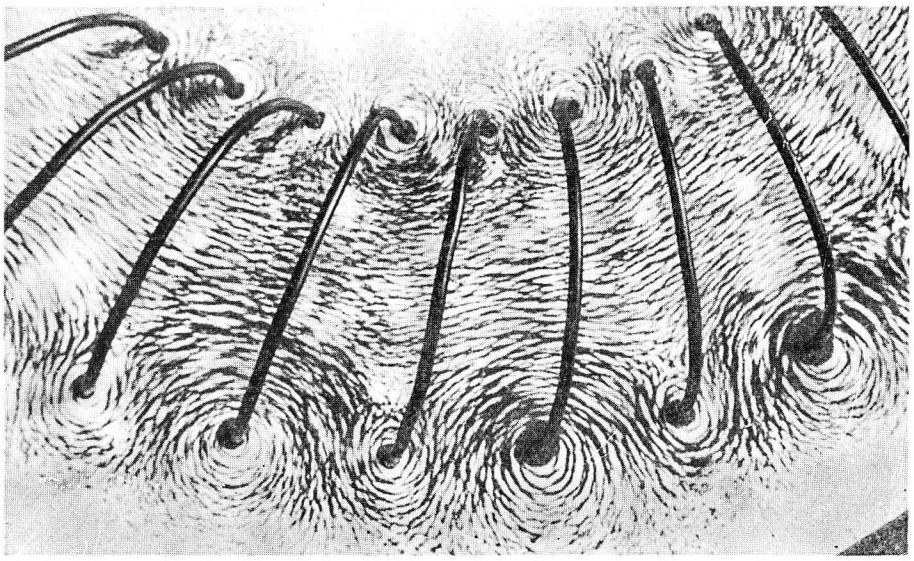

Fig. 2.16. The Heliotron H Magnetic Field $\lambda=0.40$.

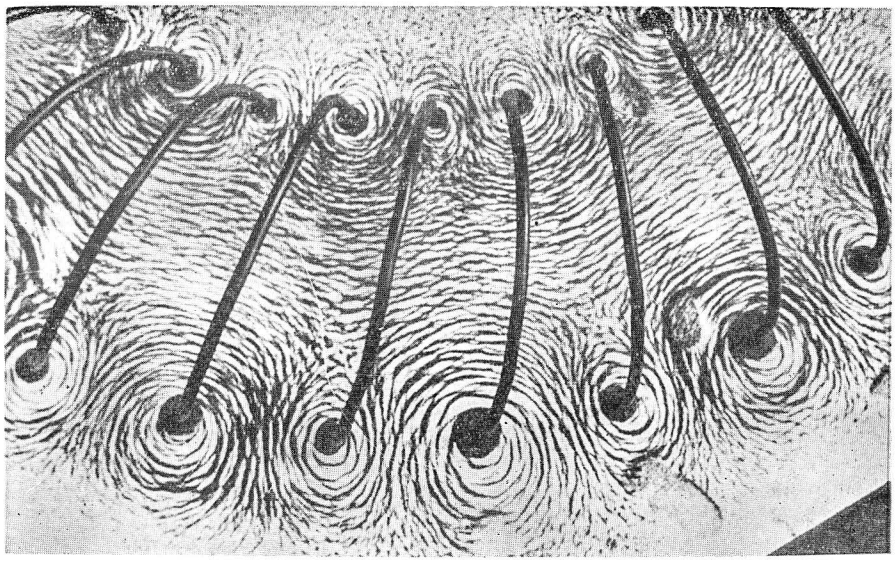

Fig. 2.17. The Heliotron H Magnetic Field $\lambda=0.67$.

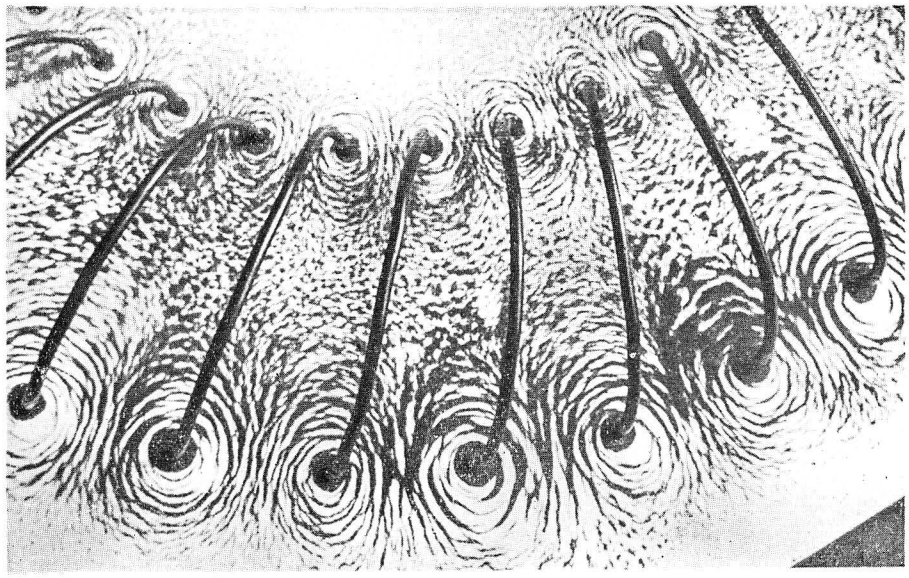

Fig. 2.18. The Heliotron H Magnetic Field $\lambda=1.00$.
(Vhe Helical Picket Fence Field)

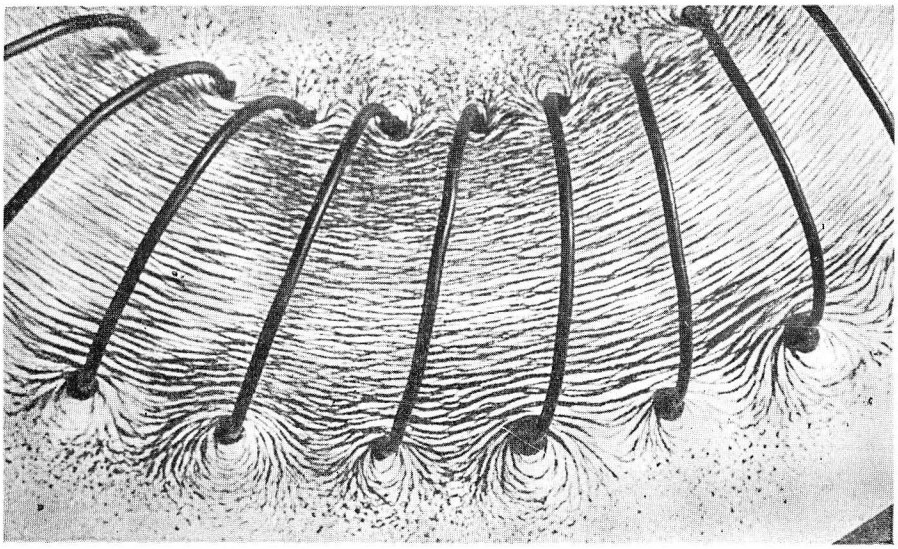

Fig. 2.19. The Heliotron H Magnetic Field $\lambda=-0.67$.
(The Toroidal Solenoid Field)

§3. Basic Equations of the Cylindrical Magnetic Field

If we assume that a cylindrical magnetic field is generated by the coils wound around a cylindrical tube and no current exists inside of it, we have

$$\text{rot}\,\boldsymbol{B}=0\,. \tag{3.1}$$

Then the magnetic flux density $\boldsymbol{B}$ is given by

$$\boldsymbol{B}=\text{grad}\,\phi\,, \tag{3.2}$$

where ϕ is a scalar function. From (3.1) and (3.2) we have

$$\nabla^2\phi=0\,, \tag{3.3}$$

and if we solve this Laplace equation we obtain $\boldsymbol{B}$ from (3.2). Equation (3.3) may be expressed in cylindrical coordinates $(\rho.\ \theta,\ z)$ as

$$\frac{\partial^2\phi}{\partial\rho^2}+\frac{1}{\rho}\frac{\partial\phi}{\partial\rho}+\frac{1}{\rho^2}\frac{\partial^2\phi}{\partial\theta^2}+\frac{\partial^2\phi}{\partial z^2}=0\,. \tag{3.4}$$

Let us assume ϕ in the following form:

$$\phi=F(\rho)G(\theta)S(z)\,, \tag{3.5}$$

where $S(z)$ and $G(\theta)$ are periodic functions of z and θ respectively. Substituting (3.5) into (3.4) and solving the resultant ordinary differential equations, we have the following solution (see Appendix II):

$$\phi = e_1 \log \rho + e_2\theta + e_3 z + \sum_{\nu=1}^{\infty}\sum_{n=0}^{\infty} \{c_\nu \cos(\nu\kappa z) + d_\nu \sin(\nu\kappa z)\}(P_n \cos n\theta + Q_n \sin n\theta) \times \{A_n I_n(\nu\kappa\rho) + B_n K_n(\nu\kappa\rho)\} \tag{3.6}$$

where $e_1 \log \rho$, $e_2\theta$ and $e_3 z$ are particular solutions of (3.4), and κ, c_ν, d_ν, P_n, Q_n, A_n and B_n are numerical constants. If we impose the boundary conditions

$$\left.\begin{aligned} |\boldsymbol{B}| &\neq \infty \quad \text{for} \quad \rho = 0, \\ B_\rho &= 0 \quad \text{for} \quad n\theta + \nu\kappa z = m\pi, \ m = 0, 1, 2, \cdots, \end{aligned}\right\} \tag{3.7}$$

to (3.6), ϕ becomes

$$\phi = e_3 z + \sum_{\nu=1}^{\infty}\sum_{n=0}^{\infty} A_{n\nu} I_n(\nu\kappa\rho) \sin(n\theta + \nu\kappa z). \tag{3.8}$$

Substituting (3.8) into eq. (3.2) we have

$$B_\rho = \kappa \sum_{\nu=1}^{\infty}\sum_{n=0}^{\infty} \nu A_{n\nu} I_n'(\nu\kappa\rho) \sin(n\theta + \nu\kappa z), \tag{3.9}$$

$$B_\theta = \frac{1}{\rho} \sum_{\nu=1}^{\infty}\sum_{n=0}^{\infty} n A_{n\nu} I_n(\nu\kappa\rho) \cos(n\theta + \nu\kappa z), \tag{3.10}$$

$$B_z = e_3 + \kappa \sum_{\nu=1}^{\infty}\sum_{n=0}^{\infty} \nu A_{n\nu} I_n(\nu\kappa\rho) \cos(n\theta + \nu\kappa z), \tag{3.11}$$

and the magnetic lines of force are obtained by solving the following differential equation:

$$\frac{d\rho}{B_\rho} = \frac{\rho d\theta}{B_\theta} = \frac{dz}{B_z}. \tag{3.12}$$

§4. Epuations for the Heliotron *B* Magnetic Field

Putting

$$n = 0, \tag{4.1}$$

in (3.9)~(3.11), we have the expression for the axisymmetrical magnetic field of the Heliotron *B* type as follows:

$$\left.\begin{aligned} B_\rho &= \kappa \sum_{\nu=1}^{\infty} \nu A_{0\nu} I_1(\nu\kappa\rho) \sin(\nu\kappa z), \\ B_\theta &= 0, \\ B_z &= e_3 + \kappa \sum_{\nu=1}^{\infty} \nu A_{0\nu} I_0(\nu\kappa\rho) \cos(\nu\kappa z). \end{aligned}\right\} \tag{4.2}$$

The magnetic field given by (4.2) approximately expresses the situation in the region inside the curve *AMB* of Fig. 2.5. Taking the simplest case,

$$\nu = 1 \tag{4.3}$$

in (4.2), we have

$$\left.\begin{aligned} B_\rho &= \kappa A_{01} I_1(\kappa\rho) \sin \kappa z\,, \\ B_z &= e_3 + \kappa A_{01} I_0(\kappa\rho) \cos \kappa z\,. \end{aligned}\right\} \tag{4.4}$$

Expression (4.4) can also be derived from the vector potential given by Lüst and Schlüter[2].

Now we take (4.4) as an approximate expression of the Heliotron B magnetic field. First we have to determine the integration constants κ, e_3, A_{01}. The assumption that the field is periodic in the z direction gives (see Fig. 4.1)

$$\kappa = \pi/a\,. \tag{4.5}$$

Putting

$$\alpha = (\pi/a)z\,, \quad \beta = (\pi/a)\rho\,, \tag{4.6}$$

(4.4) becomes

$$\left.\begin{aligned} B_\rho &= \kappa A_{01} I_1(\beta) \sin \alpha\,, \\ B_z &= e_3 + \kappa A_{01} I_0(\beta) \cos \alpha\,. \end{aligned}\right\} \tag{4.7}$$

In order to determine the constants A_{01} and e_3, we have to calculate the intensity of the magnetic field along the axis of the coils as shown in Fig. 4.1. The coils have the common radium b and their centres are located on the z axis at equal intervals a. The electric currents in these coils are I and $-\lambda I$ alternately.

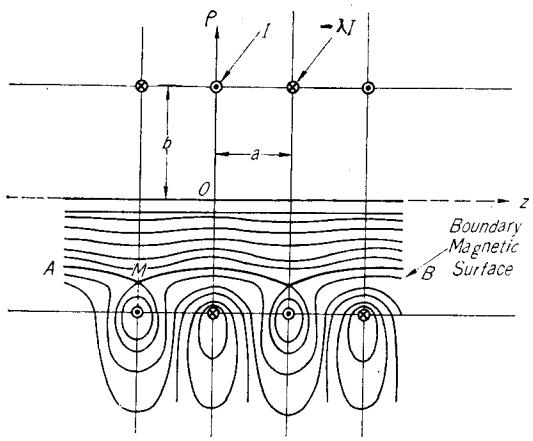

Fig. 4.1

The magnetic flux density along the axis due to a single coil placed at the origin is

$$B_{0z} = (\mu_0 b^2 I/2)(b^2+z^2)^{-3/2}\,.$$

Therefore the flux density along the axis due to all coils is given by

$$B_{0z} = \frac{\mu_0 b^2 I}{2} \sum_{\nu=-\infty}^{\infty} \left[\{b^2+(z-2\nu a)^2\}^{-3/2} - \lambda \{b^2+(z-\overline{2\nu+1}\,a)^2\}^{-3/2} \right]. \tag{4.8}$$

Let the flux density at the origen $(0,0)$ and at the point $(0,a)$, be B_{00} and B_{0a} respectively. They are given by

$$\left.\begin{aligned} B_{00} &= \{\mu_0 b^2 I/(2a^3)\}(S_1-\lambda S_2)\,, \\ B_{0a} &= \{\mu_0 b^2 I/(2a^3)\}(S_2-\lambda S_1)\,, \end{aligned}\right\} \tag{4.9}$$

where

$$\left.\begin{aligned} S_1 &= \frac{a^3}{b^3}\left\{1+\frac{b^3}{4a^3}\frac{1}{\sqrt{\left(1+\frac{b^2}{4a^2}\right)^3}}+\frac{b^3}{a^3}\left(0.0505-0.0035\frac{b^2}{a^2}+\cdots\right)\right\}, \\ S_2 &= \frac{2}{\sqrt{\left(1+\frac{b^2}{a^2}\right)^3}}+\left(0.1036-0.0107\frac{b^2}{a^2}+\cdots\right). \end{aligned}\right\} \tag{4.10}$$

B_{00} and B_{0a} are determined by (4.9) and (4.10) if the aspect ratio of the coils a/b and the current ratio λ are given. From (4.7) we have

$$e_3 = \frac{1}{2}(B_{00}+B_{0a}) = \frac{\mu_0 b^2 I}{4a^3}(S_1+S_2)(1-\lambda)\,, \tag{4.11}$$

$$B_e = \kappa A_{01} = \frac{1}{2}(B_{00}-B_{0a}) = \frac{\mu_0 b^2 I}{4a^3}(S_1-S_2)(1+\lambda)\,. \tag{4.12}$$

Denoting the coodinates of the eqilibrium point M by $[\rho_e, (2n+1)a]$ in the (ρ, z) coordinates or $[\beta_e, (2n+1)\pi]$ in the (β, α) coordinates, we have, from (4.7),

$$e_0 = I_0(\beta_e) = \frac{e_3}{\kappa A_{01}} = \frac{1-\lambda}{1+\lambda}\frac{S_1+S_2}{S_1-S_2}. \tag{4.13}$$

The position of the equilibrium point is also dependent upon a/b and λ. Substituting (4.12) and (4.13) into (4.7), we have

$$\left.\begin{aligned} B_\rho &= B_e I_1(\beta)\sin\alpha\,, \\ B_z &= B_e\{I_0(\beta_e)+I_0(\beta)\cos\alpha\}\,. \end{aligned}\right\} \tag{4.14}$$

Again substituting (4.14) into eq. (3.12), we obtain

$$\frac{d\rho}{dz} = \frac{d\beta}{d\alpha} = \frac{I_1(\beta)\sin\alpha}{I_0(\beta_e)+I_0(\beta)\cos\alpha}. \tag{4.15}$$

Integrating (4.15), we obtain the following equation for the line of force:

$$\cos\alpha = \frac{I_0(\beta_e)}{2I_1(\beta)}\beta\left(\frac{\beta_0^2}{\beta^2}-1\right), \tag{4.16}$$

where β_0 is the parameter which designates the line of force. For the lines of force inside the equilibrium point M, β_0 of a line of force is equal to the value of β on the lines of force at $\alpha=\pi/2$. The field represented by (4.14) and (4.16) is shown graphically in Fig. 4.2. But the solution given by (4.16) does not represent the true situation near the coil. In order to obtain a better approximation

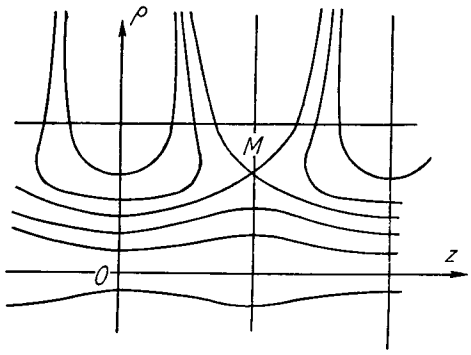

Fig. 4.2

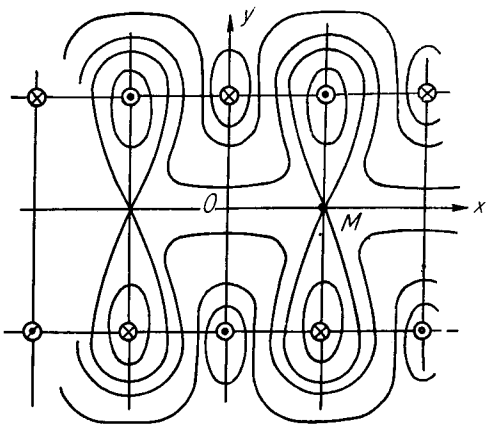

Fig. 4.3

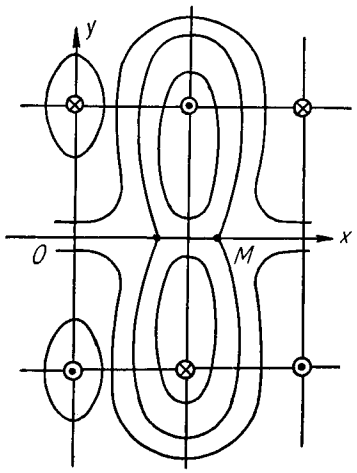

Fig. 4.4

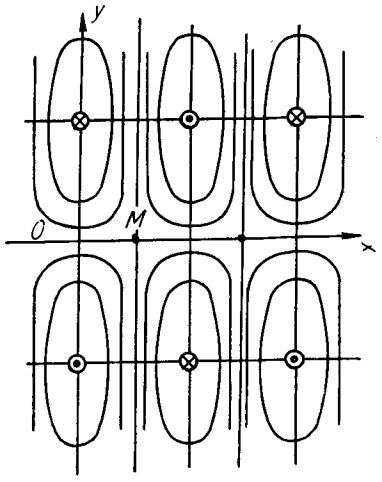

Fig. 4.5

we must compute the line of force using the complete expression (4.2). If λ tends to S_2/S_1 it may be seen from (4.13) that β_e becomes 0, that is, the equilibrium points come to the axis as shown in Fig. 4.3. Further increasing the value of λ we find that there appear two equilibrium points on the axis in one period (see Fig. 4.4). Finally for $\lambda=1$ the equilibrium points coincide with the points $\left[0, \left(n+\frac{1}{2}\right)\pi\right]$ on the axis (Fig. 4.5), and the magnetic field becomes the Picket Fence field. Figs. 4.3~4.5 have been drawn using (A.4).

§5. Cylindrical Cusp Field

The magnetic fields given by (3.9)~(3.11) include the cylindrical cusp fields as a special case. If we put, in (3.9)~(3.11),

$$\left.\begin{aligned} \nu &= 1\,, \\ \kappa z &\to 0\,, \end{aligned}\right\} \tag{5.1}$$

and expand the modified Bessel functions, we have the following expression:

$$\left.\begin{aligned} B_\rho &= \sum_{n=1}^{\infty} \frac{\kappa^n A_{n1}}{2^n(n-1)!}\,\rho^{n-1}\sin n\theta\,, \\ B_\theta &= \sum_{n=1}^{\infty} \frac{\kappa^n A_{n1}}{2^n(n-1)!}\,\rho^{n-1}\cos n\theta\,, \\ B_z &= e_3 + \sum_{n=1}^{\infty} \kappa\rho\,\frac{\kappa^n A_{n3}}{2^n(n-1)!}\,\rho^{n-1}\cos n\theta\,. \end{aligned}\right\} \tag{5.2}$$

The limit $\kappa z \to 0$ means that the period of the field in the z direction tends to infinity and in this case $\kappa\rho \to 0$. We have to ignore the term $n=0$, since this gives $B_\theta = B_\rho = 0$. For simplicity, let us take the term $n=m$ alone:

$$\left.\begin{aligned} B_\rho &= C_m \rho^{m-1}\sin m\theta\,, \\ B_\theta &= C_m \rho^{m-1}\cos m\theta\,, \\ B_z &= e_3\,, \end{aligned}\right\} \tag{5.3}$$

where

$$C_m = \kappa^m A_{m3}/\{2^m(m-1)!\}\,. \tag{5.4}$$

In (5.3) we neglected the second term of B_z as $\kappa\rho$ is assumed to be small. From (3.12) it will be seen that the projection of the line of force (5.3) to a plane perpendicular to the tube axis is represented by

$$\rho^m = \rho_0^m \left|\frac{1}{\cos m\theta}\right|\,, \tag{5.5}$$

where ρ_0 is the value of ρ at $\theta = 0$.

Figure 5.1 shows the magnetic fields in the neighbourhood of the tube axis,

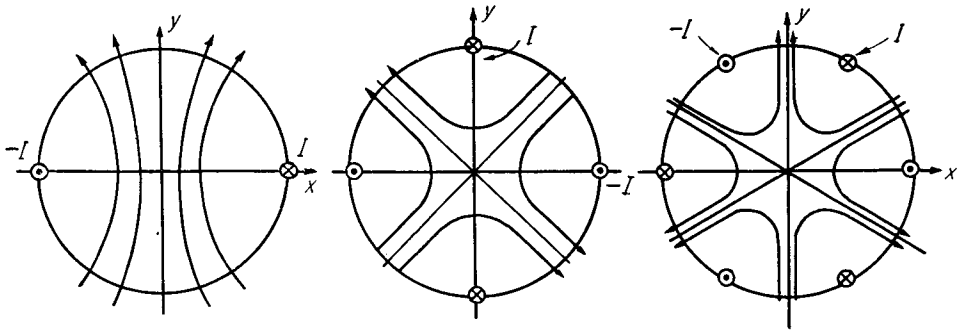

$m=1$ $m=2$ $m=3$

(a) (b) (c)

Fig. 5.1

which are given by putting $m=1$, $m=2$ and $m=3$ in (5.3) and (5.5). The magnetic fields given by (5.3) are made by superposing a constant magnetic field in the z direction upon the field which is produced by the linear currents put on the tube wall parallel to the tube axis. The flux density of the fields takes the minimum value e_3 at the axis.

Further it may be noted that the intensity of the magnetic field decreases towards the axis and thus this part of the field appears to act as a sort of magnetic bottle. However Fig. 5.1 shows that the lines of force of the field cross the tube wall, and therefore that the dilute plasma, in which particles move along the lines of force, cannot be confined within this bottle. Only the exceptional case where $e_3=0$ may yield a dense plasma which can be confined in this bottle.

§6. The Heliotron *H* Magnetic Figld (Helical Heliotron)

For $n\neq 0$, (3.9)~(3.11) give the magnetic field produced by making the coils of the Heliotron B (Fig. 2.4) helical around the tube as shown in Fig. 6.1. This

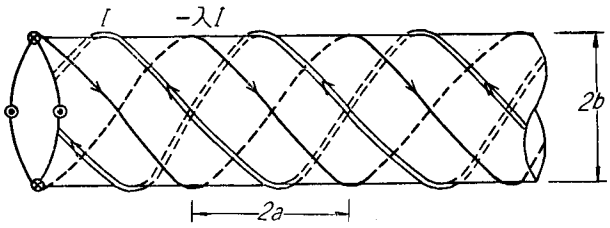

Fig. 6.1

field gives a transitional type from the Heliotron B field to the cylindrical cusp field, and it may be hoped that it will have the merits of both types of field. Putting $\nu=1$ and $n=m$ in (3.9)~(3.11), we have

$$\left.\begin{aligned} B_\rho &= \kappa A_{m1} I'_m(\beta)\sin u\,,\\ B_\theta &= \kappa A_{m1}\frac{m}{\beta} I_m(\beta)\cos u\,,\\ B_z &= e_3+\kappa A_{m1} I_m(\beta)\cos u\,, \end{aligned}\right\} \tag{6.1}$$

where

$$u = n\theta+\alpha\,. \tag{6.2}$$

Assuming that

$$\left.\begin{aligned} B_z &= 0 \quad \text{for} \quad \beta=\beta_e \quad \text{and} \quad u=\pi\,,\\ B_z &= B_0 \quad \text{for} \quad u=\frac{\pi}{2}\,, \end{aligned}\right\} \tag{6.3}$$

we have

$$e_3 = B_0\,,\quad \kappa A_{m1} = B_0/\{I_m(\beta_e)\}\,. \tag{6.4}$$

Substituting (6.4) into (6.1) we obtain

$$\left.\begin{aligned} B_\rho &= B_0\{I_m'(\beta)/I_m(\beta_e)\}\sin u\,,\\ B_\theta &= B_0(m/\beta)\{I_m(\beta)/I_m(\beta_e)\}\cos u\,,\\ B_z &= B_0\left\{1+\frac{I_m(\beta)}{I_m(\beta_e)}\cos u\right\}. \end{aligned}\right\} \tag{6.5}$$

The field given by (6.5) is produced by m pairs of helical winding. From (3.12) we have

$$\frac{d\beta}{du}=\frac{\beta B_\rho}{mB_\theta+\beta B_z}. \tag{6.6}$$

Substituting (6.5) into (6.6) we obtain

$$\left\{\beta+\left(\frac{m^2}{\beta}+\beta\right)\frac{I_m(\beta)}{I_m(\beta_e)}\cos u\right\}d\beta-\beta\frac{I_m'(\beta)}{I_m(\beta)}\sin u\,du=0\,. \tag{6.7}$$

Equation (6.7) becomes a total differential equation by multiplying by an integrating factor, and its solution is given by

$$\frac{\beta^2}{2}+\beta\frac{I_m'(\beta)}{I_m(\beta_e)}\cos u=c'\,, \tag{6.8}$$

where c' is a constant. If we assume that, along the line of force,

$$\beta=\beta_0 \qquad \text{for} \quad u=\pi/2\,, \tag{6.9}$$

we obtain the expression for the magnetic surface

$$\cos u=\frac{I_m(\beta_e)}{2I_m'(\beta)}\beta\left(\frac{\beta_0^2}{\beta^2}-1\right). \tag{6.10}$$

From (6.10) we can see that β is a function of $\cos u$ alone. This means that the lines of force inside the point ($\beta=\beta_e$. $u=\pi$) undulate in the band

$$\beta_{\min}\leqq\beta\leqq\beta_{\max}\,. \tag{6.11}$$

Therefore, if we take the field which satisfies the condition

$$\beta_e<(\pi/a)\times(\text{inner tube radius})\,, \tag{6.12}$$

the lines of force inside the equilibrium point do not cross the tube wall. An exact expression for the field produced by m pairs of helical winding is given by

$$\left.\begin{aligned} B_\rho &= \kappa\sum_{s=1}^{\infty}C_nI_n'(\beta)\sin u_n\,,\\ B_\theta &= \frac{\kappa}{\beta}\sum_{s=1}^{\infty}nC_nI_n(\beta)\cos u_n\,,\\ B_z &= e_3+\kappa\sum_{s=1}^{\infty}C_nI_n(\beta)\cos u_n\,, \end{aligned}\right\} \tag{6.13}$$

where

$$n = ms\,, \quad u_n = ms\theta + \alpha\,. \tag{6.14}$$

If we put $m=0$ in (6.10) it reduces to (4.16).

§7. Equilibrium of the Plasma in the Heliotron B Field

Under the magnetohydrodynamical approximation the equilibrium condition of the plasma is given by

$$\nabla p = \boldsymbol{j} \times \boldsymbol{B}\,, \tag{7.1}$$

where gravitational force is neglected. Equation (7.1) shows that the isobaric surfaces

$$p = \text{const}\,, \tag{7.2}$$

are woven by the lines of current and magnetic lines of force. We define a function U by the integral along the line of force

$$U = -\int \frac{dl}{B}\,, \tag{7.3}$$

where integration is carried out over one period of the line of force. We see that the isobaric surfaces coincide with the surfaces of constant U. However, assuming ϕ to be constant we have the relation

$$-U = \int \frac{dl}{B} = \frac{1}{\phi}\int dS\, dl = \frac{1}{\phi} V\,, \tag{7.4}$$

where dS is the sectional area of the infinitesimal flux tube and V is the volume involved in one period. Thus $-U$ is found to be proportional to the volume of the flux tube, and we can conclude that the isobaric surfaces coincide with the magnetic surfaces woven by the lines of force along which the volume of the flux tube is constant[3].

Furthermore in order to make the magnetic surfaces coincide with the equilibrium surfaces so as to confine the plasma, it is repuired that the isobaric surfaces be toroidal and, for practical use, be inside the toroidal discharge tube and not cross the tube wall. For example, in the case of the field produced by coils wound uniformly around a circular toroidal tube such as Zeta, the magnetic flux density B is inversely proportional to R, the distance of the line of force from the toroidal center (see Figs. 7.1 and 7.2). Then the constant U surfaces are given by

$$R = \text{const}\,. \tag{7.5}$$

The surfaces are coaxial cylinders with an axis which coincides with the toroidal axis, but they are not toroidal. Therefore, these surfaces cannot be the equili-

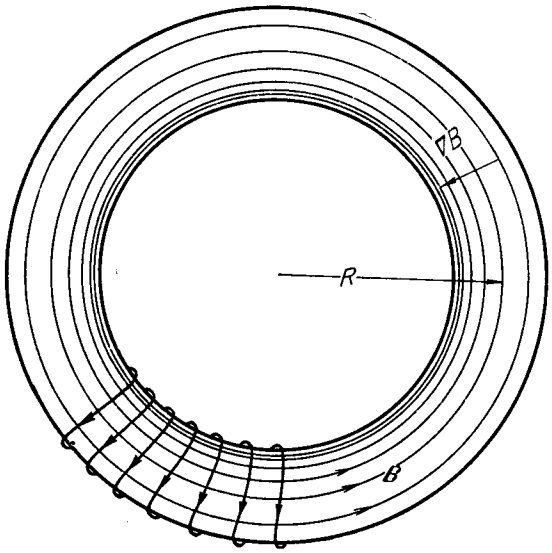

Fig. 7.1

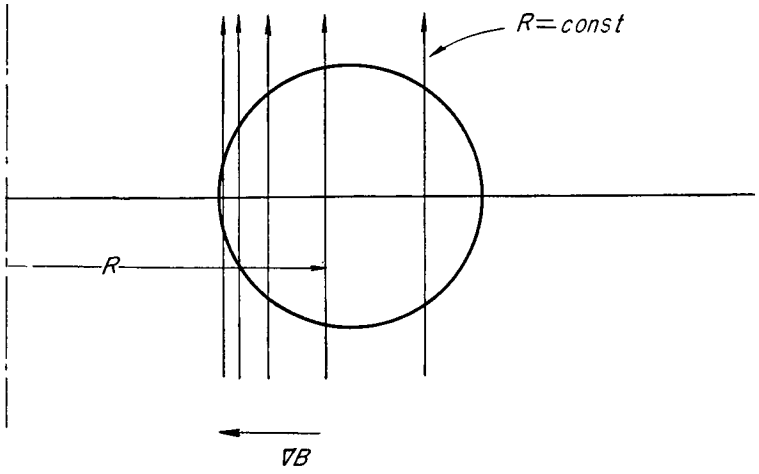

Fig. 7.2

brium surfaces. Physically, in this case, the plasma current flows in the direction of the toroidal axis and produces the charge separation which destroys the plasma confinement.

On the other hand, in the case of the undulated field, U takes different values at different distances from the tube axis. When the tube is a straight cylinder, the constant U surfaces become coaxial cylinders whose axis coincides with the tube axis. In the case of the toroidal undulated field, the surfaces be-

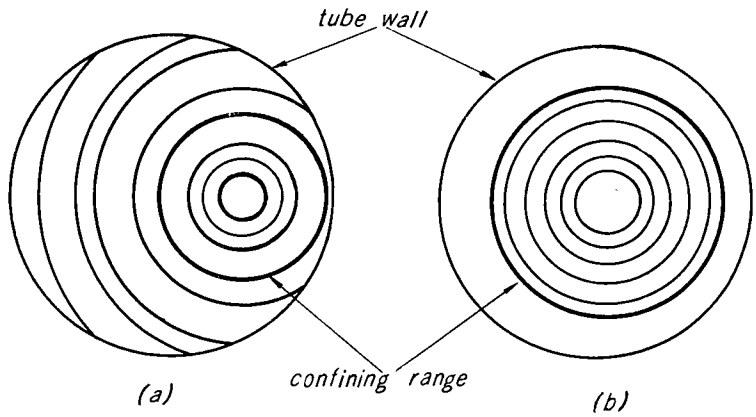

Fig. 7.3

come toroidal and their axes are different from the tube axis as shown in Fig. 7.3(a). In this case, the cross-sectional areas of the constant U surfaces which do not cross the toroidal tube wall become very small, unless one makes the toroidal radius sufficiently large compared with the tube radius or the amplitude of the undulation of the line of force sufficiently large.

The Heliotron B field, has the equilibrium points distributed periodically inside the wall. Since the flux density B becomes 0 at these points we can make U as large as we wish in the vicinity of those points. In Fig. 7.3(b), the thick solid line represents the boundary of the cross section of the magnetic surface woven by the constant U lines of force passing through the equilibrium points. In the Heliotron B field therefore, all the constant U surfaces are located inside the solid line and make toroidal surfaces. Since it is easy to have the equilibrium points inside the tube wall, it may be said that the Heliotron field essentially satisfies the necessary conditions for equilibrium.

§6. Interchange Instability of the Plasma in the Heliotron B Field

Let us consider the interchange instability[4] of the plasma confined in the Heliotron B field shown in Fig. 8.1 from the particle-dynamical point of view. In Fig. 8.1 M is an equilibrium point of the magnetic field. The change in plasma energy ΔE_p, which is caused by the interchange of the plasma contained in flux tube I with that in II of equal magnetic flux, is given by

$$\Delta E_p = -\delta N_0 \delta w_0 , \tag{8.1}$$

with

$$\delta N_0 = N_{02} - N_{01} , \tag{8.2}$$

$$\delta w_0 = \iint \delta w(\mu, \mathrm{W}) f(\mu, \mathrm{W}) d\mu dw , \tag{8.3}$$

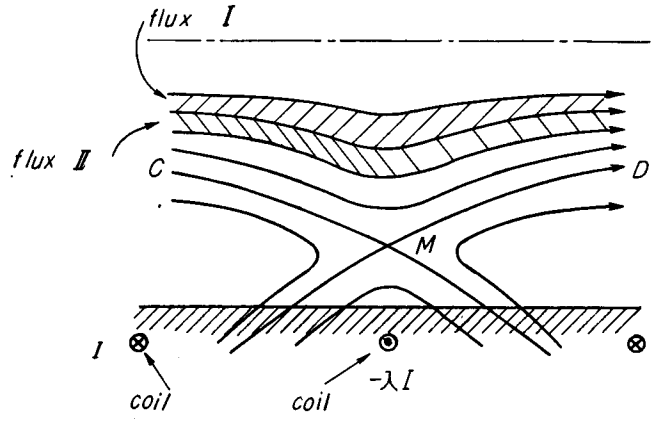

Fig. 8.1

where N_{01} and N_{02} are the number of particles contained in flux tubes I and II respectively, $\delta w(\mu, \mathrm{W})$ is the change in energy of a single particle which has magnetic moment μ and total energy W, and $f(\mu, \mathrm{W})$ is the distribution function. The condition for stability is expressed by $\Delta E_p > 0$. If $\delta w_0 > 0$ the plasma is stable for interchange instability according to the orbit theory[4], and we discuss the case $\delta w_0 < 0$. In this case the plasma cannot be stable except for the case $\delta N_0 > 0$. Now,

$$N_0 = n_0 V = n_0 k_0 \int \frac{dl}{B}, \tag{8.4}$$

where n_0 denotes the average density of the plasma in the flux tube of volume V, and k_0 is a positive constant. The condition $\delta N_0 > 0$ is reduced to

$$\delta \int \frac{dl}{B} \Big/ \int \frac{dl}{B} > -\delta n_0 / n_0 . \tag{8.5}$$

The average density n_0 must be zero on the line of force *CMD* which forms the the plasma boundary, and $\delta \int \frac{dl}{B}$ is positive inside *CMD* in the Heliotron B field. In order to examine condition (8.5), we expand (4.14) and (4.16) putting

$$\left.\begin{aligned} \alpha &= \pi + \xi, \qquad (\xi/\pi)^2 \ll 1, \\ \beta &= \beta_e - \eta, \qquad (\eta/\beta_e)^2 \ll 1, \end{aligned}\right\} \tag{8.6}$$

and we have

$$B_z = a_0(e_0 + e_1\sqrt{\xi^2 + u^2} + e_2\xi^2), \tag{8.7}$$

where a_0 is a constant and e_0, e_1, e_2 and u are functions of β_0. We put

$$Q = \int \frac{dl}{B} = k \int_0^{\pi} \frac{d\alpha}{B_z} = Q_0 + Q_1, \tag{8.8}$$

where

$$Q_0 = k\int_0^{\tau}\frac{d\xi}{B_z}, \quad Q_1 = k\int_0^{\pi-\tau}\frac{d\alpha}{B_z}, \tag{8.9}$$

and τ is a small positive constant which satisfies $(\tau/\pi)^2 \ll 0$. In the vicinity of *CMD* we find that Q_0 is very large and Q_1 a constant value Q_{10} approximately. Denote the value of β_0 on the line *CMD* by β_{0e}, then if β_0 approaches to β_{0e} we find that (see Appendix III)

$$Q \approx Q_c + \log\frac{1}{\sqrt{\beta_{0e}^2-\beta_0^2}}, \quad Q_c = \text{const} \tag{8.10}$$

and that condition (8.5) is reduced to

$$\frac{1}{n_0}\frac{\partial n_0}{\partial \beta_0} > -\frac{\beta_0}{\beta_{0e}^2-\beta_0^2}\Big/\left\{Q_c + \log\frac{1}{\sqrt{\beta_{0e}^2-\beta_0^2}}\right\}. \tag{8.11}$$

If n_0 is expressed by

$$n_0 = n_{01} = k_0\Big/\left\{Q_c + \log\frac{1}{\sqrt{\beta_{0e}^2-\beta_0^2}}\right\}^m, \qquad k_0 > 0. \tag{8.12}$$

The stability condition becomes

$$1 > m > 0. \tag{8.13}$$

If the average density distribution satisfies condition (8.11) the plasma is stable for interchange instability. But if the effect of diffusion gives a finite gradient of n_0 in the vicinity of *CMD*, the stability condition will not be satisfied and interchange instability will occur. When the plasma temperature becomes sufficiently high, the effect of diffusion becomes weaker, and we may expect that the rate of growth of instability is also very small. If we consider the azimuthal magnetic field produced by the axial plasma current, the magnetic field produced by the windings of the Heliotron B device will be twisted by this azimuthal field. As a result, the rotational transform for the magnetic field would be provided and the plasma would become stable. These questions must be clarified through future experiments with the Heliotron *B*.

The author wishes to express his gratitude to Professor S. Hayashi for his continual encouragement and to Professor C. Hayashi for his helpful advice.

References

1) Uo, K.: Kakuyūgō kenkyū, (Thermonuclear Fusion Research ... in Japanese) **1** (1958) 12, **2** (1959) 247, **3** (1959) 679.
2) Lüst, R. & Schlüter, A: Z. Naturforschg. **12** a (1957) 850.
3) Kadmtsev, B. B.: Plasma Physics and the Problem of Controled Thermonuclear Reactions, IV (1957) 17.
4) Rosenbluth, M. N. & Longmire, C. L.: Annals of Physics, **1** (1957) 120.
5) Uo, K: J. Phys. Soc. Japan Vol. 16, No. 6, (1961) 1380.
6) Uo, K.: J.I.E.E.J. Vol. 81, No. 878, Nov. (1961).

§ Appendix I

In order to investigate the qualitative features of the axisymmetric Heliotron field, we first approximate a part of the torus tube by a straight tube and then replace the magnetic field in the straight tube produced by the series of coil pairs (see Fig. 2.1) by a field produced by infinite rows of straight currents (see Fig. A.1). The vector potential of the magnetic field produced by these currents is given by

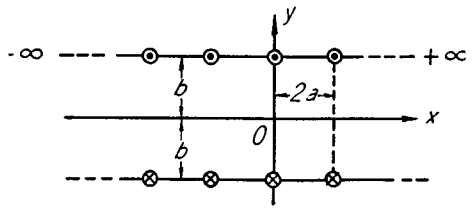

Fig. A.1

$$\left.\begin{aligned} A_{x0} &= A_{y0} = 0, \\ A_{z0} &= \frac{\mu_0 I}{4\pi} \sum_{\nu=-\infty}^{\infty} \log \frac{(x+2\nu a)^2+(y+b)^2}{(x+2\nu a)^2+(y-b)^2} \\ &= \frac{\mu_0 I}{4\pi} \log \frac{\cosh\frac{\pi}{a}(y+b)-\cos\frac{\pi}{a}x}{\cosh\frac{\pi}{a}(y-b)-\cos\frac{\pi}{a}x}. \end{aligned}\right\} \tag{A.1}$$

The equation of the line of force is expressed by

$$\cos\frac{\pi}{a}x = \cosh\frac{\pi}{a}b\cosh\frac{\pi}{a}y - \coth\zeta\sinh\frac{\pi}{a}b\sinh\frac{\pi}{a}y. \tag{A.2}$$

where ζ is a parameter which designates the line of force. Using eq. (A.2) we can draw Fig. 2.2 as the qualitative sketch of the magnetic field made by the double coil series as shown in Fig. 2.1. In similar way we can calculate the vector potential of the double current rows as shown in Figs. A.2 and A.3 respectively:

$$A_x = A_y = 0, \quad A_z = \frac{\mu_0 I}{4\pi} \log \frac{\left\{\cosh\frac{\pi}{a}(y+b)-\cos\frac{\pi}{a}x\right\}\left\{\cosh\frac{\pi}{a}(y-d)-\cos\frac{\pi}{a}x\right\}^{\lambda}}{\left\{\cosh\frac{\pi}{a}(y-b)-\cos\frac{\pi}{a}x\right\}\left\{\cosh\frac{\pi}{a}(y+d)-\cos\frac{\pi}{a}x\right\}^{\lambda}}, \tag{A.3}$$

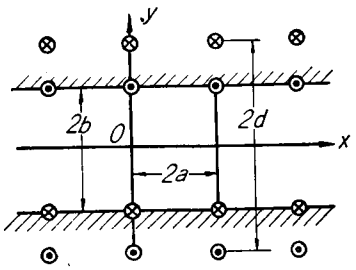

Fig. A.2

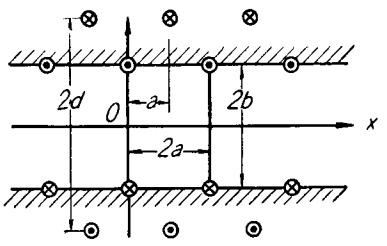

Fig. A.3

$$A_x = A_y = 0, \quad A_z = \frac{\mu_0 I}{4\pi} \log \frac{\left\{\cosh\frac{\pi}{a}(y+b)-\cos\frac{\pi}{a}x\right\}\left\{\cosh\frac{\pi}{a}(y-d)+\cos\frac{\pi}{a}x\right\}^{\lambda}}{\left\{\cosh\frac{\pi}{a}(y-b)-\cos\frac{\pi}{a}x\right\}\left\{\cosh\frac{\pi}{a}(y+d)+\cos\frac{\pi}{a}x\right\}}, \tag{A. 4}$$

These magnetic fields are shown graphically in Figs. 2.5 and 2.6.

§ Appendix II

Since $S(z)$ in (3.5) is a periodic function of z, we have

$$S(z) = \sum_{\nu=1}^{\infty} S_\nu = \sum_{\nu=1}^{\infty} \{C_\rho \cos(\nu\kappa z) + d_\nu \sin(\nu\kappa z)\}, \tag{A. 5}$$

where κ, c_ν, d_ν are constants. Substituting (3.5) and (A.5) into (3.4) we have

$$\sum_{\nu=1}^{\infty} \left\{G \cdot S_\nu \left(\frac{\partial^2 F}{\partial \rho^2} + \frac{1}{\rho}\frac{\partial F}{\partial \rho} - \nu^2\kappa^2 F\right) + \frac{F \cdot S_\nu}{\rho^2}\frac{\partial^2 G}{\partial \theta^2}\right\} = 0. \tag{A. 6}$$

Since the above equation must be satisfied for arbitrary values of z, we have the following relation

$$\frac{\rho^2}{F}\left(\frac{\partial^2 F}{\partial \rho^2} + \frac{1}{\rho}\frac{\partial F}{\partial \rho} - \nu^2\kappa^2 F\right) = -\frac{1}{G}\frac{\partial^2 G}{\partial \theta^2}, \tag{A. 7}$$

The left-hand side of the above equation is a function of ρ alone and the right-hand side of θ alone, and therefore both sides must equal a constant, n^2 say. Thus we obtain the following two equations:

$$\frac{\partial^2 F}{\partial \rho^2} + \frac{1}{\rho}\frac{\partial F}{\partial \rho} - \left(\frac{n^2}{\rho^2} + \nu^2\kappa^2\right)F = 0, \tag{A. 8}$$

$$\frac{\partial^2 G}{\partial \theta^2} + n^2 G = 0. \tag{A. 9}$$

If n is a positive integer, the general solution of eq. (A.8) is expressed by

$$F(\rho) = \sum_{n=0}^{\infty} \{A_n I_n(\nu\kappa\rho) + B_n K_n(\nu\kappa\rho)\}, \tag{A. 10}$$

and that of eq. (A.9) is given by

$$G(\theta) = \sum_{n=0}^{\infty} (P_n \cos n\theta + Q_n \sin n\theta). \tag{A. 11}$$

Substituting (A.5), (A.10) and (A.11) into (3.5) and adding simple particular solutions of eq. (3.4), we obtain the solution (3.6).

§ Appendix III

Substituting (8.6) into (4.14) and expanding it we obtain

$$B_z = a_0\left(a_1\eta - a_2\eta^2 + \frac{1}{2}\xi^2 + \cdots\right) \tag{A. 12}$$

where

$$\left.\begin{aligned} &a_0 = B_e I_0(\beta_e)\,,\quad a_1 = I_1(\beta_e)/I_0(\beta_e)\,,\\ &a_2 = (1/2)(1-a_1/\beta_e)\,. \end{aligned}\right\} \tag{A. 13}$$

In the same way, from eq. (4. 16) we have

$$\frac{\xi^2}{u^2}-\frac{(\eta-p)^2}{v^2} = -1\,, \tag{A. 14}$$

where

$$\left.\begin{aligned} p &= g_1\zeta/(1-g_2\zeta)\,,\\ u^2 &= 2g_0\zeta\left\{1+\frac{g_1^2}{2g_0(1-g_2\zeta)}\zeta+\frac{g_1^2}{2(1-g_2\zeta)}\zeta^2\right\},\\ v^2 &= u^2/\{(1-g_2\zeta)(1+g_0\zeta)\}\,, \end{aligned}\right\} \tag{A. 15}$$

$$\left.\begin{aligned} g_0 &= 1/(2a_1\beta_e)\,,\\ g_1 &= 1\Big/\left\{(2a_1^2\beta_e)\left(1+\frac{1}{2a_1\beta_e}\zeta\right)\right\},\\ g_2 &= \left(1-\frac{a_1}{2\beta_e}\right)\Big/\left\{a_1^3\beta_e\left(1+\frac{1}{2a_1\beta_e}\zeta\right)\right\}, \end{aligned}\right\} \tag{A. 16}$$

and

$$\zeta = \beta_{0e}^2-\beta_0^2\,. \tag{A. 17}$$

β_{0e} is the value of β_0 of the line of force passing through the equilibrium point. Eliminating η in (A. 12) by using (A. 14), we have (8. 7), and where

$$\left.\begin{aligned} e_0 &= p(a_1-a_2p)-a_2v^2\,,\\ e_1 &= (v/u)(a_1-2a_2p)\,,\\ e_2 &= (1/2)-a_2v^2/u^2\,. \end{aligned}\right\} \tag{A. 18}$$

Putting in (8. 9)

$$x = \nu\sqrt{\xi^2+u^2}\,,\quad u_0 = \nu\sqrt{u^2+\tau^2}\,, \tag{A. 19}$$

reduces to

$$Q_0 = \frac{2}{a_0e_2\kappa}\int_0^{u_0}\frac{dx}{x^2+(e_1/e_2)x+(e_0/e_2-u^2)}\frac{1}{\sqrt{x^2-u^2}}dx\,. \tag{A. 20}$$

Q_0 is expressed by

$$\left.\begin{aligned} Q_0 &= \frac{2}{a_0e_2\kappa}\frac{1}{x_1-x_2}(Q_{01}-Q_{02})\,,\\ Q_{01} &= \frac{x_1}{\nu\sqrt{u^2-x_1^2}}\left\{\frac{\pi}{2}+Tan^{-1}\frac{x_1u_0-u^2}{\nu\sqrt{(u^2-x_1^2)\tau^2}}\right\},\\ Q_{02} &= \frac{x_2}{\nu\sqrt{x_2^2-u^2}}\log\left[\frac{(u-x_2)\{(x_2u_0-u^2)-\nu\sqrt{(x_2^2-u^2)(u_0^2-u^2)}\}}{(u_0-x_2)(x_2-u)u}\right], \end{aligned}\right\} \tag{A. 21}$$

where x_1 and x_2 are the roots of the following equation:

$$x^2+(e_1/e_2)x+(e_0/e_2-u^2) = 0\,. \tag{A. 22}$$

When ζ becomes very small, Q_0 is approximately expressed by (8. 10).